Short Papers

Complex Correction of Data Acquisition Channels Using FIR Equalizer Filters

István Kollár and Yves Rolain

***Abstract*—The common conviction about FIR (finite impulse response) digital filters is that the number of necessary taps, to reach the same performance as provided by IIR (infinite impulse response) digital filters, is usually too large. Moreover, the standard FIR filter design algorithm (Remez exchange) allows the design of linear-phase filters only. Therefore, IIR filters are often preferred over FIR ones, without any further investigations.**

This paper presents a case study of complex (amplitude and phase) equalization of the passband of a commercial anti-aliasing filter. The novelty is the usage of an FIR filter for this purpose (or an FIR one, combined with a low-order IIR filter), and a thorough discussion of the special design aspects.

It turns out that for the given anti-aliasing filter (a Cauer filter of order 11) an FIR filter of length 60 · · · 100 can perform as well as a 26/26 (numerator order/denominator order) IIR one. The properties are even better if a low-order IIR filter is used in combination with an FIR one (orders, e.g., 1/1 + 40/0). Because of the absence of stability problems and the ease of implementation, the use of FIR filters is suggested.

***Keywords*—Equalization, compensation, signal conditioning, data acquisition channel, correction filter, digital filter design, FIR filter approximation in complex domain.**

I. Introduction

Anti-aliasing filters are used in most data acquisition channels to suppress undesirable high-frequency input signal components. These filters always have some passband amplitude error, and usually a significant phase distortion (see, e.g., Fig. 1). These errors are even subject to component tolerances.

With the appearance of powerful signal processors, it became possible to equalize the passband transfer function at the digital side [1]–[4], by implementing an appropriate digital compensation filter. Since the transfer function is usually modeled by an s-domain or z-domain rational form, the "natural" way for this equalization is the design of IIR compensation filters. FIR filters are usually not used, because of the common conviction that FIR filters need a too large number of taps for good performance. As we will see in the following sections, the latter statement does not generally hold. Considering further that FIR filters have no stability problems (instability is maybe the major difficulty in IIR filter design), and that the implementation of FIR filters is very straightforward, it is worthwhile to use them whenever the specifications are met by a reasonably low-order filter.

In this paper the same data acquisition channel will be considered as for the IIR compensation in [1] and [2]. We will try to reduce the relative complex error:

$$e_{\mathrm{dB}} = 20 \cdot \log \frac{|tf| + |e|}{|tf|} \tag{1}$$

where tf is the transfer function, and e is the complex error of the fit at a given frequency. To make a fair comparison of the methods, we will compensate the passband up to 19.6 kHz, as it was also done in [1] and [2].

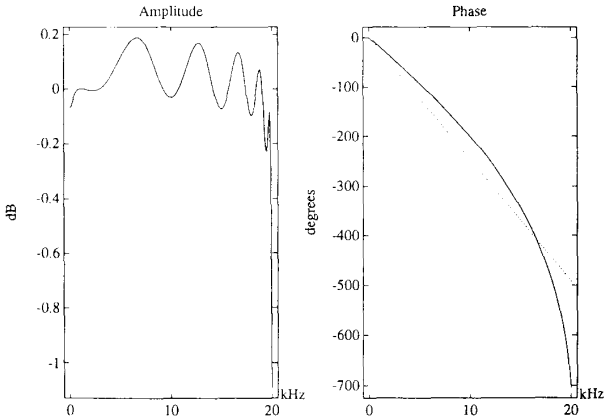

Fig. 1. Passband of the anti-aliasing filter to be compensated. The filter is a Cauer low-pass filter of order 11.

II. Design Aspects of FIR Compensation Filters

The digital filter

1) should correct the anti-aliasing filter for gain variations and phase nonlinearity in the passband,
2) should not introduce too large gains elsewhere (stopband and transition band),
3) should have minimal order, to allow implementation at low cost and high speed (a low order means further that the impulse response will be short, a desirable feature in time-domain applications), and
4) should be designed using an effective algorithm which does not demand too much computing time and requires minimal human intervention.

Let us discuss these aspects one by one.

A. Passband Error

Numerical methods usually approximate the desired frequency response at discrete frequencies only. Since high-order FIR filters contain a lot of free parameters, the discrete frequencies must be chosen densely enough to avoid wild oscillations between neighboring points. A rule of thumb [4] is to use four times as many frequency points for the design than the number of the FIR coefficients, which means that we have about eight times more real equations than parameters.

Manuscript received July 20, 1992; revised April 2, 1993.

I. Kollár is with the Department of Measurement and Instrument Engineering, Technical University of Budapest, H-1521 Budapest, Hungary.

Yves Rolain is with Dienst ELEC, Vrije Universiteit Brussel, B-1050 Brussels, Belgium.

IEEE Log Number 9210523.

There is an important practical limitation to the decrease of the residual error of the compensation. If a transfer function, which is not smooth, is to be compensated (see, e.g., the one in Fig. 1 near 20 kHz), the compensated transfer function can be very sensitive to small changes of the original one (e.g., due to aging or thermal drift). This is illustrated in Fig. 2: 0.01% (100 ppm) increase in the sampling frequency (or a similar change in the parameters of the anti-aliasing filter itself) results in a rather large compensation error near 20 kHz (about 100 mdB complex error). This fact implies that *the input channel of an instrument should always be designed as a whole*, since hardware-dependent parameters like the ratio of the highest passband frequency to the sampling frequency, the type of the anti-aliasing filter, etc. already determine the possible minimum error of the compensation.

B. Stopband Gain

The relatively large number of degrees of freedom may give rise to large stopband gains. Since a complex function is to be fitted, the passband behavior of the anti-aliasing filter contains information concerning also the stopband. This is even more apparent in the case of Fig. 1, where near the edge of the passband the filter already starts to attenuate. This means that the correction filter will also try to invert a part of the transition band (and maybe part of the stopband), and will therefore have a *large stopband gain*. This can be avoided by artificially introducing zero transfer function points in the stopband, with a reasonably small weight in order to allow acceptable deviations from zero, compared to the desired small passband error. These stopband zero points have to be defined in a sufficient number, in order to avoid that the algorithm just puts zeros to each zero value. The zero points must also be close enough to each other, and cover possibly the whole stopband.

C. Filter Order and Allowed Delay

The necessary order of the FIR filter depends on the desired accuracy and on the shape of the transfer function to be inverted. The proper filter length can be chosen by trial and error, or by theoretical considerations [7]. The goal may be to have a minimum compensation error for an acceptable filter length, or to have a compensation error smaller than a given limit, using the minimum number of taps. A small filter length is desirable, even if the hardware allowed the implementation of longer filters in real time, since the design time for the filter increases progressively with the number of taps.

When using digital compensation filters, a certain delay also has to be allowed. This means that the filtered data will appear delayed with respect to the ideally compensated data, or in z-domain terms, we have to approximate

$$z^{-\tau}H_{\text{des}}(z), \quad \text{instead of} \quad H_{\text{des}}(z) \tag{2}$$

where $H_{\text{des}}(z)$ is the desired (inverse) transfer function, z^{-1} is the unity delay operator, and τ is the normalized delay. This delay is usually acceptable in data acquisition channels (it is also present in the IIR filters designed in [1] and [2]). The value of τ also has to be optimized; the best value is often around $1/3$–$1/2$ times the filter order [14].

D. Effective Algorithm

As it is seen from (1), the fit is to be performed in the complex domain. Unfortunately, the classical, very effective Parks–McClellan (Remez exchange) algorithm [9] works either for the real or the imaginary case only, producing a linear-phase FIR filter,

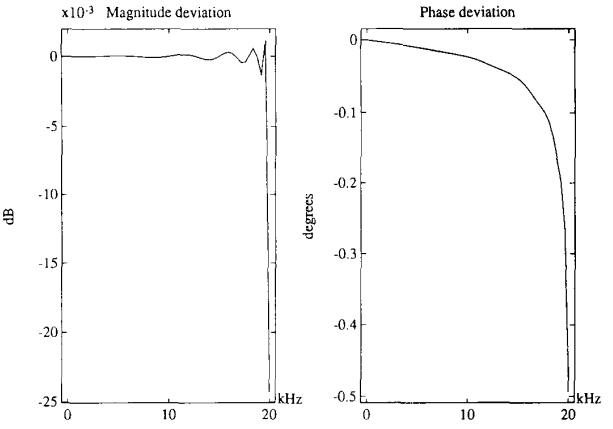

Fig. 2. Theoretical error of the ideal compensation when the sampling frequency increases by 0.01% (100 ppm).

fitted in minimax sense. For the complex case solutions exist, but there is still no generally accepted algorithm. Preuss [10] introduced a generalized version of the Parks–McClellan algorithm for the complex case. Nagy [8] used the Remez exchange algorithm to fit the real and imaginary parts of the transfer function separately, combined them to a nonlinear-phase FIR filter (this brought the obtained design error under $\sqrt{2}$ times the optimum one), and used an iterative scheme to reach the minimax fit. Leeb and Henk [11] used Padé approximant techniques in an iterative scheme, based on the Remez exchange algorithm. Ellacott and Williams [12] used the reweighted LS technique (RWLS). Mason and Chit [13] described another RWLS technique, based on ideas of the least mean square (LMS) technique, used in control theory. Chen and Parks [14] transformed the complex-domain problem into an approximately equivalent linear programming one, and solved this latter using Algorithm 495 [15]. It is also possible to use the minimum p-error method of Deczky [16], originally developed for the design of IIR filters, or optimal Hankel-norm approximations [7].

In order to find the best way of the filter design, the different algorithms should be compared systematically with respect to their speed, memory need, convergence for high orders, etc. before making a choice. This may be the topic of future research. However, since we have ready-to-use programs for the weighted least squares (WLS) fitting, we used a modified version of the RWLS technique, which converged rapidly.

III. Design Results

In [1] and [2] the design of IIR compensation filters for the equalization of the input channel of a dynamic signal analyzer was described. In this section, FIR filters will be designed for the same purpose, with the same specification.

In [1] the original 0.2 dB amplitude error and about 50° phase error were reduced to 10 mdB and 0.066°, respectively, using a 34/34 order IIR filter. In [2] it was shown that the above design is not optimal, and 26/26 filter was designed with the same performance.

For the design of the FIR filters, we used the identification result of [1] as a reference function. Since its modeling error is about 3 mdB, we allow 7 mdB fitting error. About 150 complex amplitudes are used in the total band, providing $2 \times 150 = 300$ real equations.

An FIR filter of order 56 (57 taps) has fitting errors smaller than 7 mdB, and a filter of length 49 performs better than 10 mdB. The filters are easily realizable (see Fig. 3), and provide an acceptable

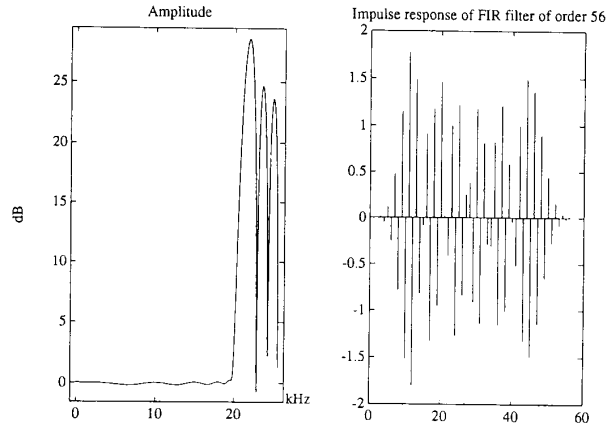

Fig. 3. Amplitude response and impulse response of the FIR filter of length 56.

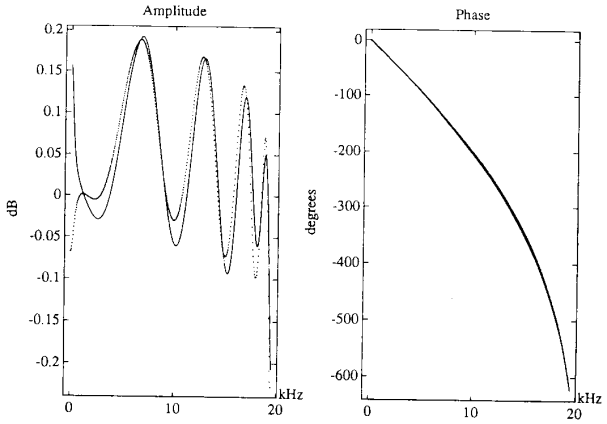

Fig. 4. Measured passband behavior of two anti-aliasing filters.

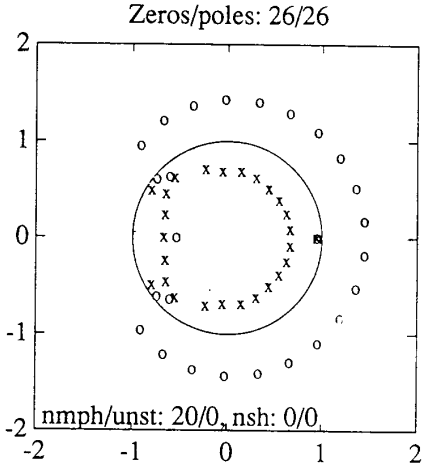

Fig. 5. Pole-zero pattern of the 26/26 IIR compensation filter [2].

stopband gain. It is interesting to observe that, because of the allowed 30 dB stopband gain, the impulse response has a high-pass character.

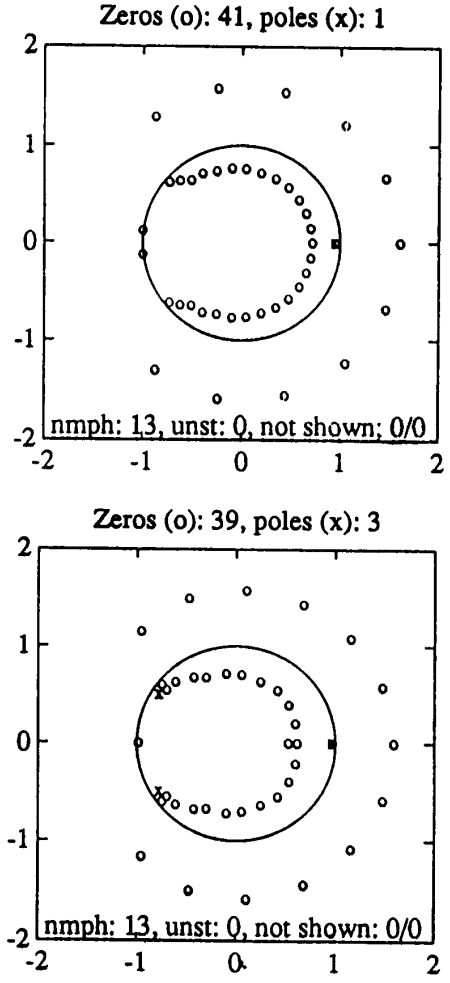

Fig. 6. Pole-zero patterns of the 41/1 and 39/3 compensation filters.

TABLE I
COMPARISON OF THE NECESSARY ORDERS OF THE DIFFERENT DESIGNS FOR THE SAME ERROR

	IIR	FIR	Mixed FIR-IIR	
Order	26/26	56/0	41/1	39/3
Delay (taps)	26.56	17	17	18

Experimenting with other anti-aliasing filter boards of the same type, it turned out that though their global behavior is very similar, sometimes the FIR order, necessary to obtain 7 mdB fitting error, is much larger (>100). Fortunately, this number is still acceptable for real-time implementation at $f_s = 51.2$ kHz. We observed that in these cases the initial WLS design is definitely worse at low frequencies. This may be due to the different behavior under 1 kHz (Fig. 4), which seems to be the consequence of a small impedance mismatch at the input of the anti-aliasing filter. Nevertheless, the IIR method still worked fine without an increase in the order (its error is not more than 7 mdB); thus we speculated that the worse FIR performance was due to a pole, close to the unit circle. Indeed, a pole/zero pair near $z = 1$ (see Fig. 5) is in the first case $p_1 = 0.94686$, $z_1 = 0.94629$, while in the second case $p_2 = 0.96776$, z_2

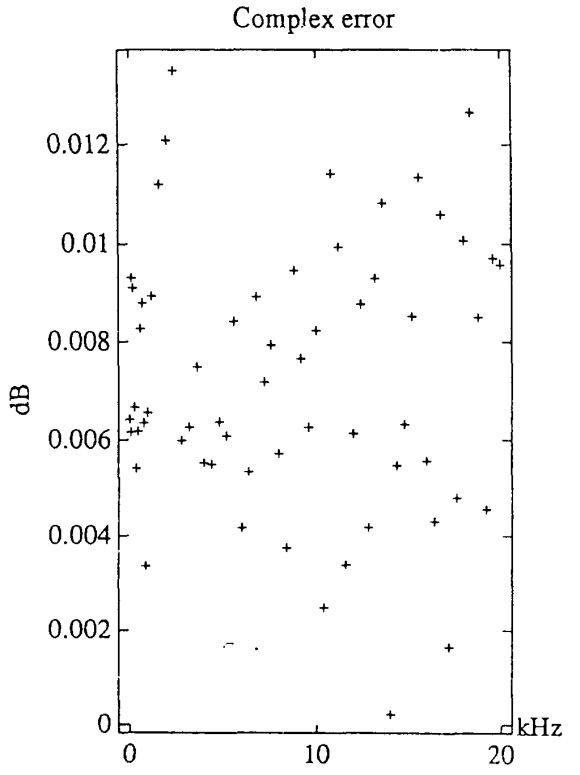

Fig. 7. Measured complex error of the data acquisition channel after compensation.

$= 0.96828$. The second pole is significantly closer to the unit circle than the first one:

$$(1 - p_1)/(1 - p_2) \approx 0.053/0.032 = 1.65.$$

The closer the pole to the unit circle, the more zeros are necessary to define a similar transfer function. This puts a limit to the applicability of the FIR filters for compensation.

A. Mixed FIR-IIR Structure

Based on the above observation, a "mixed" strategy can also be applied: when the resulting FIR order is too high, and there are stable poles close to the unit circle, the corresponding pole/zero pairs can be realized in low-order IIR sections, and the rest of the compensation can be done by an FIR filter. It can be observed in Fig. 5 that there are altogether three poles quite close to the unit circle: one at $z = 1$, and two near the edge of the passband (at approximately 21 kHz). Thus it is worth trying to fit the desired function by an FIR filter, combined with 1/1 and 3/3 IIR ones.

The results of the design are presented in Table I (see also Fig. 6). The elimination of the two complex poles does not bring a dramatic change in the order, but elimination of the real one does. The total number of coefficients (42×2) is even lower than that of the IIR filter ($27 + 27 = 54$).

IV. Experimental Verification

The FIR compensation filter, designed by the above-described methods, was implemented in the input channel of a signal analyzer (DSA710). Fig. 7 shows the measured complex error after compensation: it illustrates well that the deterministic error (which is covered by random measurement errors) is not more than about 10 mdB, since the 95% confidence limit of the random error is about 1–2 mdB [1]. Based on the above results, the IIR compensation filter has been replaced by an FIR one in the DSA710.

V. Conclusions

It has been illustrated via the example of a dynamic signal analyzer that it is possible to improve the quality of data acquisition channels by means of surprisingly low-order FIR correcting filters, instead of IIR ones. In contrast to the common opinion, the necessary FIR orders are not very high at all. An even more advantageous approach is the use of a mixed structure: the poles located the closest to the unit circle in the z-plane are realized in low-order precompensating IIR section(s), and the rest of the compensation is then possible with an FIR filter of much lower order. Clearly, the use of FIR filters is preferable because of the absence of stability problems and the ease of the implementation, at least if the desired error reduction can be achieved by an acceptable filter length.

Acknowledgment

The authors gratefully acknowledge very useful remarks and suggestions of Rik Pintelon and Johan Schoukens (Vrije Universiteit Brussel), those of Ferenc Nagy (Technical University of Budapest), and further, the measurement data provided by Danny De Valk (Spinnov N.V., Belgium).

References

[1] R. Pintelon, Y. Rolain, M. Vanden Bossche, and J. Schoukens, "Towards an ideal data acquisition channel," *IEEE Trans. Instrum. Meas.*, vol. 39, pp. 116–120, Feb. 1990.

[2] I. Kollár, R. Pintelon, Y. Rolain, and J. Schoukens, "Another step towards an ideal data acquisition channel," *IEEE Trans. Instrum. Meas.*, vol. 40, pp. 659–660, June 1991.

[3] I. Kollár, R. Pintelon, Y. Rolain, and J. Schoukens, "Equalization of data acquisition channels using digital filters," *Periodica Polytechnica Ser. Elect. Eng.*, vol. 34, no. 3, pp. 167–178, 1990.

[4] J. Schoukens and R. Pintelon, *Identification of Linear Systems: A Practical Guideline to Accurate Modelling*. Oxford, UK: Pergamon, 1991.

[5] J. Schoukens, R. Pintelon, and J. Renneboog, "Maximum likelihood estimation of the parameters of linear systems," *Periodica Polytechnica Ser. Elect. Eng.*, vol. 33, no. 4, pp. 165–182, 1989.

[6] R. Pintelon and J. Schoukens, "Robust identification of transfer functions in s- and z-domain," *IEEE Trans. Instrum. Meas.*, vol. 39, no. 4, pp. 565–573, Aug. 1990.

[7] K. Glover, "All optimal Hankel-Norm approximations of linear multivariable systems and their L^∞-error bounds," *Int. J. Control*, vol. 39, no. 6, pp. 1115–1193, 1984.

[8] F. Nagy, "Signal conditioning and reconstruction in telemetry systems by means of digital filtering," in *Proc. Europe. Telemetry Conf.* ETC'90, Garmisch-Partenkirchen, Germany, May 1990, pp. 132–139.

[9] J. H. McClellan, T. W. Parks, and L. R. Rabiner, "FIR filter design and synthesis," In *Programs for Digital Signal Processing*. New York: IEEE Press, pp. 5.1-1–5.1-13.

[10] K. Preuss, "On the design of FIR filters by complex Chebyshev approximation," *IEEE Trans. Acoust., Speech, and Signal Proc.*, vol. 37, pp. 702–712, May 1989.

[11] F. Leeb and T. Henk, "Simultaneous amplitude and phase approximation for FIR filters," *Int. J. Circuit Theory and Appl.*, vol. 17, pp. 363–374, 1989.

[12] S. Ellacott and J. Williams, "Linear Chebyshev approximation in the complex plane using Lawson's algorithm," *Math. Comp.* vol. 30, no. 133, pp. 35–44, Jan. 1976.

[13] J. S. Mason and N. N. Chit, "New approach to the design of FIR digital filters," *IEE Proceedings*, vol. 134, pt. G, no. 4, pp. 167–180, Aug. 1987.

[14] X. Chen and T. W. Parks, "Design of FIR filters in the complex domain," *IEEE Trans. Acoust., Speech, and Signal Processing*, vol. ASSP-35, pp. 144–153, Feb. 1987.
[15] I. Barrodale, "ALGORITHM 495: Solution of an overdetermined system of linear equations in the Chebyshev norm," *ACM Trans. Math. Software*, vol. 1, no. 3, pp. 264–270, Sept. 1975.
[16] A. G. Deczky, "Synthesis of recursive digital filters using the minimum p-error criterion," *IEEE Trans. Audio and Electroacoustics*, vol. AE-20, pp. 257–263, Oct. 1972.

On the Four-Frequency Measurement Process for Coupled Dual Resonator Crystals

David A. Roberts and Gerald E. Roberts

***Abstract*—A simplified derivation of the basic four-frequency measurement process for a coupled dual resonator crystal is given which shows a more direct path than previously published for obtaining the two resonator frequencies either from the poles and zeros of $1/y_{11}$ or from the zeros of $1/y_{11}$ and the zeros of z_{11}, the latter of which tends to be the more useful. Using the resonator frequencies obtained from either of the two cases, the synchronous peak separation frequency (SPSF) is obtained by recognizing that**

$$\omega_A^2\omega_B^2 - A_{22} = 1/(L_1L_2C_{12}^2).$$

I. Introduction

One of the most useful measurement processes developed over the past two decades is the four-frequency process for measuring coupled dual resonator crystals [1]–[3]. The process provided for the first time an accurate, yet simple, method for determining the three key parameters needed in the fabrication of a coupled dual crystal after the formation of the resonators on the crystal plate. These key parameters are the two resonator frequencies and the intrinsic coupling between resonators, the latter of which is called the synchronous peak separation frequency (SPSF). As part of this measurement process, a method was developed which also allows one for the first time to determine SPSF when the two resonator frequencies are not equal. Several other important features of this measurement process are 1) that only one of the two ports of a coupled dual crystal need be monitored to obtain the specific four frequencies needed to calculate the two resonator frequencies and SPSF, 2) that the basic measurement fixture needs no tuning, and 3) that the two resonator frequencies and SPSF can be accurately determined at any step during the crystal fabrication after the formation of the resonators on the crystal plate.

In this paper, a simplified derivation of the basic measurement process is given to show a more direct path from the short-circuit and open-circuit driving-point impedances, $1/y_{11}$ and z_{11}, of a coupled dual resonator crystal to the four measured frequencies and then to the two resonator frequencies and SPSF.

Manuscript received October 23, 1992.
D. A. Roberts is a student at Duke University's School of Engineering, Durham, NC 27706.
G. E. Roberts is with Ericsson GE Mobile Communications, Inc., Lynchburg, VA 24502.
IEEE Log Number 9211486.

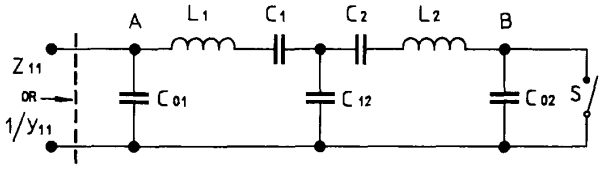

Fig. 1. Equivalent circuit of a coupled dual resonator crystal for determining the driving-point impedance z_{11} when switch S is open and the driving-point impedance $1/y_{11}$ when switch S is closed.

II. Peaks and Valleys

From Fig. 1, the driving-point admittance y_{11} of the input port or the A-side of the crystal with the output port or B-side short-circuited, i.e., switch S closed, is

$$y_{11} = I_1/V_1 \quad \text{with} \quad V_2 = 0. \tag{1}$$

By determining y_{11}, it is seen that

$$y_{11} = C_{01}s + [(L_2C_1C_2C_{12})s^3 + (C_1C_2 + C_{12}C_1)s]/[(L_1L_2C_1C_2C_{12})(s^4 + A_{11}s^2 + A_{22})] \tag{2}$$

where

$$A_{11} = (L_1C_1C_2 + L_1C_1C_{12} + L_2C_2C_{12} + L_2C_1C_2)/(L_1L_2C_1C_2C_{12}) \tag{3}$$

$$= 1/(L_2C_{12}) + 1/(L_2C_2) + 1(L_1C_1) + 1/(L_1C_{12}) \tag{4}$$

$$A_{22} = (C_1 + C_2 + C_{12})/(L_1L_2C_1C_2C_{12}). \tag{5}$$

From (2)–(5), it is seen that the form of the driving-point impedance $1/y_{11}$ is then

$$1/y_{11} = (s^4 + A_{11}s^2 + A_{22})/[C_{01}s(s^4 + B_{11}s^2 + B_{22})] \tag{6}$$

$$= (s^2 + \omega_{SC1}^2)(s^2 + \omega_{SC3}^2)/[C_{01}s(s^2 + \omega_{SC2}^2)(s^2 + \omega_{SC4}^2)] \tag{7}$$

where ω_{SC1} and ω_{SC3} are the zeros of $1/y_{11}$, and ω_{SC2} and ω_{SC4} are the poles. If $1/y_{11}$ is displayed via the voltage divider circuit in Fig. 2, then ω_{SC1} and ω_{SC3} show up as the frequencies of the voltage resonances, or peaks, at the output of the voltage divider and ω_{SC2} and ω_{SC4} as the voltage antiresonances, or valleys, where

$$\omega_{SC1} < \omega_{SC2} < \omega_{SC3} < \omega_{SC4}. \tag{7}$$

From (6), it is seen that

$$A_{11} = \omega_{SC1}^2 + \omega_{SC3}^2 \tag{8}$$

$$A_{22} = \omega_{SC1}^2\omega_{SC3}^2 \tag{9}$$

are obtained from the short-circuit peaks, and

$$B_{11} = \omega_{SC2}^2 + \omega_{SC4}^2 \tag{10}$$

$$B_{22} = \omega_{SC2}^2\omega_{SC4}^2 \tag{11}$$

are obtained from the short-circuit valleys.

By inverting y_{11} in (6) and dividing the resulting numerator by the denominator, then y_{11} can be put in the form

$$y_{11} = C_{01}s + C_{01}(B_{11} - A_{11})(s^3 + [B_{22} - A_{22}]s/[B_{11} - A_{11}])/(s^4 + A_{11}s^2 + A_{22}). \tag{12}$$